Direct measurement of the *in vitro* hemoglobin content of erythrocytes using the photo-thermal effect of the heme group

Bong Seop Kwak,[a] Beom Seok Kim,[a] Suk-Heung Song,[a] Hyun Ok Kim,[b] Hyung Hee Cho[a] and Hyo-Il Jung*[a]

Received 14th April 2010, Accepted 19th June 2010
DOI: 10.1039/c0an00235f

Blood hemoglobin is an important diagnostic parameter in measuring overall health. The hemoglobin molecule and the iron it contains absorb light energy, leading to thermal changes. This paper presents a new method for determining the hemoglobin concentration of erythrocytes by measuring temperature increases of the heme group when cells are heated by a 532 nm wavelength laser. The advantages of our method are that it determines the hemoglobin content of an entire blood sample without chemical treatments and requires only a small amount of blood (less than 10 μL). A micro scaled platinum resistance temperature detector (Pt RTD) was fabricated using a microelectromechanical system (MEMS) technique that directly measures the temperature changes. The platinum RTD's resistance at 0 °C is 275.32 Ω. For the specific heating of erythrocytes, we used a 0.03 to 9.6 W cm^{-2} power tunable diode pumped solid state (DPSS) continuous wave (CW) laser module with a wavelength of 532 nm. When heating human erythrocytes, leukocytes, plasma, and reference solutions, only the temperature of the erythrocytes significantly increased, indicating that our measurement technique can be used to determine hemoglobin concentration. The hemoglobin concentrations for the samples we used were 0.34, 0.67, 1.35, 2.7, 5.4, 8.1, 10.8, 13.5, 16.2, 18.9 and 21.6 g dL^{-1}. The temperatures measured for each sample were 31.17 ± 1.98, 36.34 ± 3.76, 42.70 ± 4.38, 48.39 ± 6.47, 63.73 ± 3.34, 79.09 ± 9.60, 84.86 ± 1.99, 87.54 ± 9.84, 91.90 ± 5.27, 90.00 ± 3.24 and 95.79 ± 2.66 °C at a 9.6 W cm^{-2} output power of the 532 nm laser at 23 °C. We also provide a theoretical analysis of the temperature increases and investigate their major heat source.

Introduction

Blood is an important connective tissue and is used frequently for clinical diagnoses. Much emphasis has been placed on the diagnosis of blood-related diseases such as HIV, AIDS, malaria, anemia, and diabetes using biochemical methods such as dyeing, DNA analysis, and antigen–antibody techniques. The hemoglobin concentration of erythrocytes is an important clinical indicator to diagnose anemia patients as insufficient hemoglobin concentration can lead to oxygen transportation decline. In addition, infections by malaria-inducing *Plasmodium falciparum* cause structural, biochemical, and mechanical modifications to host red blood cells (RBCs), leading to the digestion of considerable amounts of hemoglobin by the parasites.[1] Changes in hemoglobin concentration can lead to alterations in membrane deformability and may cause metabolic changes, cardiovascular disorders, neurological disorders, endocrinological disorders, or hepatobiliary disease.[2] In cases of hemorrhage by operation or injury, the concentrations of hemoglobin have to be monitored in order to maintain oxygen homeostasis.[3] Dialysis patients, premature births which require significant amounts of blood for diagnostic testing, and women with heavy hemorrhaging during pregnancy and menstruation require continuous monitoring of their hemoglobin concentration.

[a]*School of Mechanical Engineering, Yonsei University, 262 Seongsan-no Seodaemun-gu, Seoul, 120-749, Republic of Korea. E-mail: uridle7@yonsei.ac.kr; Fax: +82-2-312-2159; Tel: +82-(0)2-2123-5814*
[b]*College of Medicine, Yonsei University, 262 Seongsan-no Seodaemun-gu, Seoul, 120-749, Republic of Korea*

The existing methods for measuring hemoglobin concentrations include the hemoglobin cyanide (cyanmethemoglobin, HiCN) method,[4] hematocrit, and absorbance measured at the isobestic wavelength.[5] In the cyanide methemoglobin method, the erythrocyte's lipid bilayer is destroyed to release hemoglobin. Then, cyanide hemoglobin is produced through cyanization and is subjected to light of a specific wavelength, as depicted in Fig. 1. Although the conventional colorimetric measurement is the standard method promoted by the International Committee for Standardization in Hematology (ICSH), toxic chemicals such as potassium cyanide (KCN) and dimethyllaurylamine oxide (DMLAO) must be used. The hematocrit method requires a large quantity of blood for centrifugal separation of the erythrocytes. The absorption difference method, while noninvasive, is also not very accurate. Motivated by these limitations, we introduce a new technique for measuring hemoglobin concentration using the photo-thermal effect. Conventional colorimetric analysis and our photo-thermal method are compared in Fig. 1. It is generally known that chromophores absorb photons of specific wavelengths and convert them to thermal energy.[6] Wavelength, pulse duration, and pulse energy are the important variables in the photo-thermal effect,[7,8] but wavelength is the major factor in determining photo-thermal efficiency. For example, hemoglobin molecules absorb 418 nm, 530–545 nm, and 577–595 nm wavelength photons and convert this energy to thermal energy. Especially, the 532 nm wavelength has an absorption peak and the photothermal parameters of erythrocytes at this wavelength are well known from previous studies.[4,8–10] Similarly, water and melanosome absorb 2.94 μm, 10.6 μm and 520–530 nm,

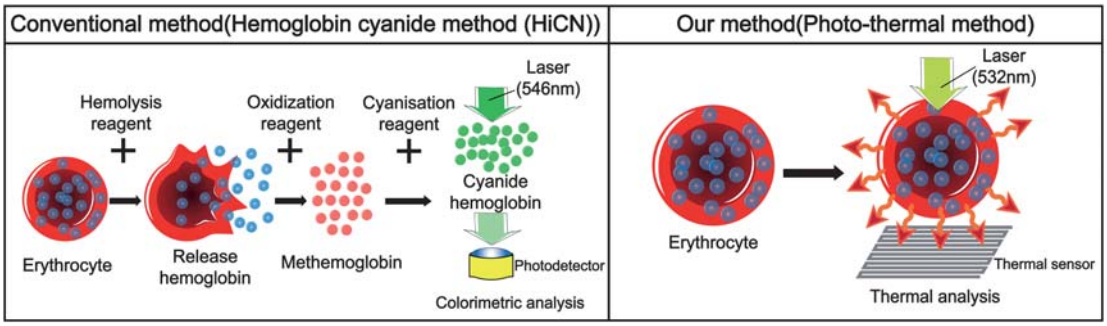

Fig. 1 Comparison of a conventional technique (the hemoglobin cyanide method) with our photo-thermal method. The hemoglobin cyanide method uses toxic chemical reagents to extract the hemoglobin out of the red blood cell. On the other hand, the photo-thermal method measures hemoglobin concentration without pretreatment.

600–700 nm wavelength photons, respectively. Pulse duration and energy are proportional to the temperature changes in the target molecules,[9] meaning a time-resolved laser module must be used to reduce the heat injury near the target.[10] However, time-resolved laser modules are large scale, expensive and require trained personnel to operate, analyze, and maintain the system.

In this paper, we describe the design, fabrication, and operation of a novel micro-scale system focused on hemoglobin concentration measurement using the photo-thermal effect, as shown in Fig. 1. Photon energy is applied *via* a tunable 532 nm continuous wave laser module to activate thermal changes in the erythrocytes, and the selective thermal change in the erythrocyte sample is measured on a micro-fabricated platinum temperature sensor chip.

Experimental section

Fabrication of the micro-resistive temperature detector (RTD)

Resistive temperature detectors (RTDs) are thermometers used to measure temperature by correlating the resistance changes of the RTD element with temperature changes. Platinum is a precious metal with the most stable and linear resistance/temperature relationship, making it very useful in these types of systems.[11–13] The Callendar–Van Dusen eqn (1, 2) can be used to describe this relationship.

For temperatures between −200 °C and 0 °C the equation is

$$R(t) = R(0)[1 + A \times t + B \times t^2 + (t - 100)C \times t^3] \quad (1)$$

while for temperatures between 0 °C and 661 °C it becomes

$$R(t) = R(0)(1 + \mathrm{A} \times t + \mathrm{B} \times t^2) \quad (2)$$

In these equations, $R(t)$ represents the resistance at temperature t, and A, B, and C are constants of the material used. For platinum, A, and B are 3.833×10^{-3}, and -3.607×10^{-9}, respectively. The constants were experimentally measured. Since B is relatively small, the resistance changes are almost linear with temperature. The sensitivity is determined by the resistance at 0 °C. We applied a four-wire Pt RTD configuration, which further increases the accuracy and reliability of the resistance

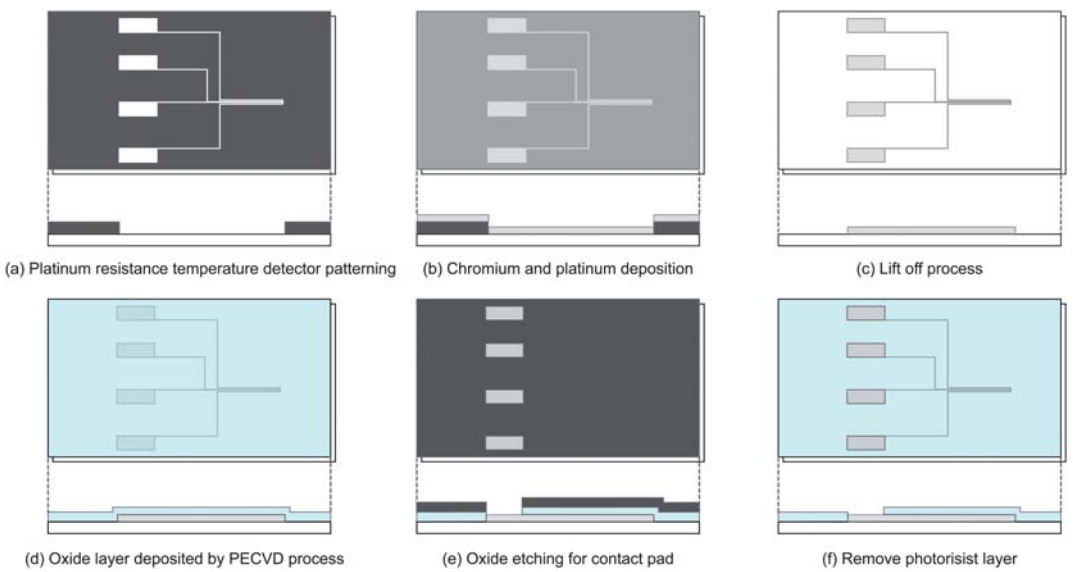

Fig. 2 The fabrication process for the micro-thermo-chip. (a) Spin coating and UV patterning of the photoresistance layer. (b) Platinum deposition on the ultra thin chromium adhesion layer. (c) Lift off process. (d) Silicon dioxide deposition for preventing unwanted resistance changes in a conductive solution. (e) Silicon dioxide etching of the contact pad. (f) Removing the photoresistance layer.

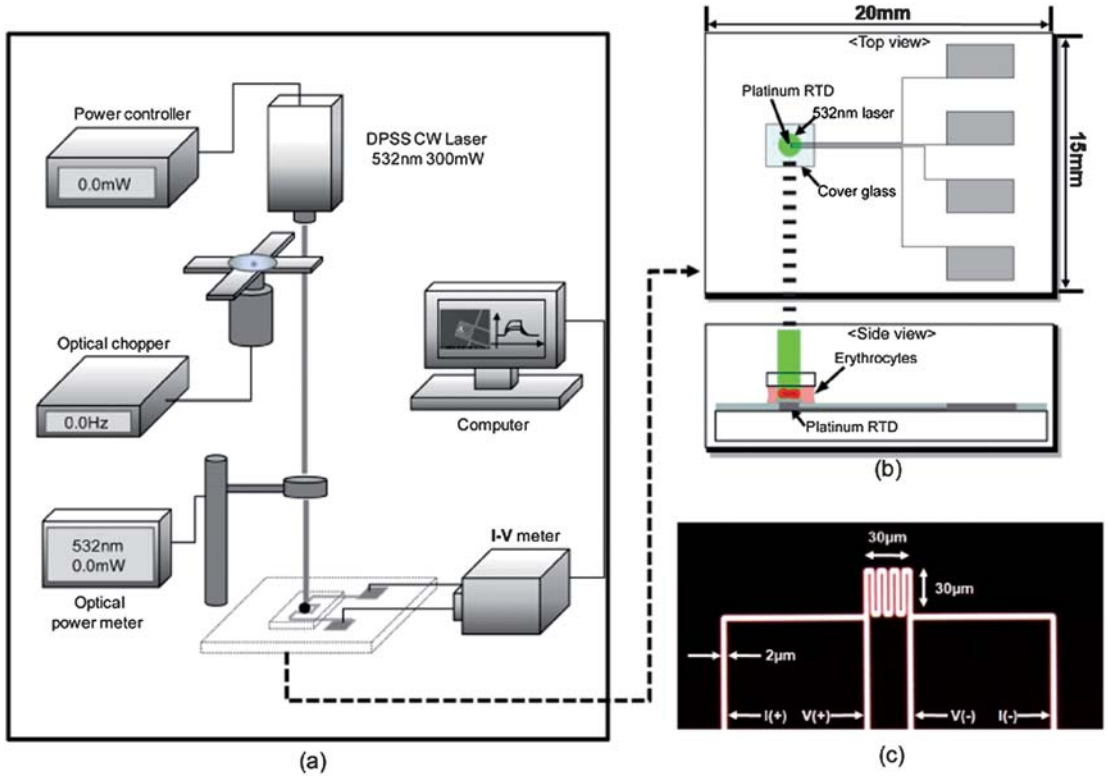

Fig. 3 (a) The experimental setup. (b) Top and side views of the micro-thermo-chip in the experimental scheme. (c) A photographic image of the micro-fabricated platinum resistance temperature detector.

being measured by providing full cancellation of resistance error due to spurious effects and lead wire resistance.[14] As shown in Fig. 3(c), the outer set of wires is used as the current path, and the inner set is used for the voltage measurement. We fabricated micro-platinum RTDs on a glass wafer using a conventional photolithography and lift-off process as shown in Fig. 2. To prepare the device, two photomasks are required: one to construct the platinum electrodes, and the other to devise a contact pad for connecting to the measurement equipment. First, an AZ5214 (Clariant Industries Ltd.) image reverse photosensitive polymer layer was spin coated at 2500 rpm onto a Pyrex 7740 (Thomas Eng., Ltd.) glass wafer. This Pyrex glass wafer is suitable for micro thermal sensors and possesses thermal shock resistance, lower thermal conductivity (1.005 W mK^{-1}) than silicon (148 W mK^{-1}), and a low thermal expansion coefficient (32.5 $\times$ 10^{-7} $^{\circ}C^{-1}$). Second, double exposure was performed using a 365 nm wavelength Karl Suss MA6 Mask Aligner, 14 mJ cm^{-2}) for 2.1 s and 13 s for the negative image of the photoresist layer. Third, the developing process was completed using an AZ300 (Clariant Industries Ltd.) developer for 26 s. Fourth, 200 Å chromium (Cr) and 1000 Å 99.99% purity platinum (Pt) were consecutively deposited onto the surface of the Pyrex glass wafer, patterned with an image-reverse photoresist layer using E-beam evaporator equipment. Note that the ultra-thin chromium layer is necessary to improve the adhesion between the Pyrex glass wafer and the platinum layer. After deposition, the lift-off process was performed using acetone, and a very thin oxide layer (1000 Å) was deposited by plasma-enhanced chemical vapor deposition (PECVD) to prevent resistance changes due to particle contact with the sensing area. The fabricated micro Pt RTD is shown in Fig. 3(c).

Experimental setup

A 532 nm wavelength laser module (power tunable from 1 to 300 mW, continuous wave, diode pumped solid state) was equipped vertically as shown in Fig. 3(a). The laser beam diameter at the aperture was 2.0 mm. The power stability of the laser module was less than 3% over four hours. The output power of the laser is controlled by an electric current. An XYZ-stage was employed for laser focusing onto the device. For accurate laser irradiation, we measured the output power of the beam using an optical power meter (PM100, Thorlabs). The uncertainty of laser power was less than $\pm$0.5%. The on/off state of the laser beam was controlled by an optical chopper system (MC1000A-optical chopper system, MC1F2-2slot blade, Thorlabs). The distance between the laser source and the device was 157 mm. The resistance changes of the micro-fabricated platinum RTD were measured by an *I–V* meter (National Instrument PXI-4071 DMM, PXI-4130 power SMU, PXI-1033 chassis). Also, a Faraday cage was used for noise cancellation and reduced the interfering electromagnetic waves from the surrounding environment.

Blood sample preparation

The two most widely used types of cell culture media for blood cells and one biological buffer solution were chosen. Blood cell media consisting of DMEM (Dulbecco's Modified Eagle's

Table 1 Experimental conditions and the resulting temperature changes

Bioanalyte									
Variable	Target sample	Cell density/10^6 cells μL^{-1}	Hemoglobin concentration/g dL^{-1}	1.6 W cm^{-2}/°C	3.2 W cm^{-2}/°C	4.8 W cm^{-2}/°C	6.4 W cm^{-2}/°C	8.0 W cm^{-2}/°C	9.6 W cm^{-2}/°C
Control	Platinum RTD	N/A	0	23.81 ± 0.11	25.14 ± 0.21	26.50 ± 0.39	27.78 ± 0.65	29.06 ± 0.84	30.34 ± 1.01
Cell culture media	RPMI	N/A	0	24.83 ± 0.08	25.74 ± 0.29	26.61 ± 0.60	27.44 ± 0.83	28.46 ± 1.31	29.45 ± 1.31
	PBS	N/A	0	25.14 ± 0.13	26.16 ± 0.08	27.18 ± 0.29	28.14 ± 0.47	29.40 ± 0.73	30.21 ± 0.68
	DMEM	N/A	0	24.26 ± 0.05	25.46 ± 0.39	26.50 ± 0.63	27.54 ± 0.92	28.69 ± 1.30	29.61 ± 1.54
Whole blood	Blood plasma	N/A	0	26.21 ± 0.21	26.97 ± 0.05	27.73 ± 0.37	28.48 ± 0.66	29.29 ± 1.04	29.89 ± 1.28
	Leukocyte	Buffy coat	Less than 0.3	26.94 ± 0.05	28.30 ± 0.05	28.74 ± 0.06	29.87 ± 0.06	30.86 ± 0.05	32.24 ± 0.05
	Erythrocytes	0.12	0.34	25.41 ± 0.45	26.53 ± 0.36	27.57 ± 0.13	28.69 ± 0.55	29.74 ± 1.18	31.17 ± 1.98
		0.23	0.67	26.21 ± 0.73	28.25 ± 0.50	30.41 ± 0.11	32.32 ± 0.86	34.48 ± 2.22	36.34 ± 3.76
		0.45	1.35	26.76 ± 0.89	30.13 ± 0.99	33.44 ± 0.44	36.62 ± 0.47	39.39 ± 2.04	42.70 ± 4.38
		0.91	2.70	27.28 ± 2.35	30.60 ± 3.47	35.68 ± 1.54	41.19 ± 2.71	44.68 ± 5.06	48.39 ± 6.47
		1.81	5.40	29.94 ± 0.14	37.48 ± 1.78	44.61 ± 3.42	50.48 ± 4.86	56.61 ± 4.67	63.73 ± 3.34
		2.72	8.10	32.81 ± 0.68	44.34 ± 0.97	53.89 ± 1.54	62.71 ± 2.58	71.47 ± 6.27	79.09 ± 9.60
		3.62	10.80	31.51 ± 0.63	44.81 ± 0.45	55.41 ± 1.40	66.54 ± 1.20	76.30 ± 3.52	84.86 ± 1.99
		4.53	13.50	33.75 ± 0.65	45.54 ± 2.40	58.01 ± 4.57	68.68 ± 6.73	78.78 ± 8.32	87.54 ± 9.84
		5.44	16.20	33.41 ± 0.67	47.63 ± 1.10	60.05 ± 2.22	71.55 ± 2.48	83.63 ± 3.89	91.90 ± 5.27
		6.35	18.90	34.69 ± 0.50	47.01 ± 2.01	59.01 ± 3.68	70.54 ± 4.46	81.07 ± 4.62	90.00 ± 3.24
		7.24	21.60	33.96 ± 0.18	47.68 ± 1.13	59.66 ± 2.17	71.14 ± 2.55	82.98 ± 3.18	95.79 ± 2.66

Medium, DMEM with 10% (v/v) FBS and 1% (v/v) penicillin streptomycin), RPMI (Roswell Park Memorial Institute medium, RPMI 1640 with 10% (v/v) FBS and 1% (v/v) penicillin streptomycin), and PBS solution (phosphate buffered saline, 137 mM NaCl, 10 mM phosphate, 2.7 mM KCl, pH 7.4) were used. The blood samples were collected from a healthy male in his twenties. All experiments were performed in compliance with the relevant laws and institutional guidelines, and the blood samples were obtained from all voluntary donors with written informed consent. In order to prevent coagulation, liquid K_3EDTA (Lavender BD Vacutainer®) was used. The erythrocytes which were used to measure the photo-thermal effect difference between leukocytes and blood plasma were separated from the blood sample using a centrifuge (Centrifuge MF80, Hanil Science Industrial) operated at 2000 rpm for 10 min. The hemoglobin concentration of the prepared blood sample was validated using a conventional hematology system (ADVIA®2120). We collected leukocytes (buffy coat) and plasma from the same human blood using centrifugation. The hemoglobin concentration of the AB plasma was validated at 0 g dL^{-1} using the same conventional hematology system. Different concentrations of hemoglobin were prepared using centrifugal separtion of erythrocytes. The erythrocytes were enriched by plasma removal and were diluted using AB plasma to create several concentration levels: 0.34 g dL^{-1}, 0.67 g dL^{-1}, 1.35 g dL^{-1}, 2.7 g dL^{-1}, 5.4 g dL^{-1}, 8.1 g dL^{-1}, 10.8 g dL^{-1}, 13.5 g dL^{-1}, 16.2 g dL^{-1}, 18.9 g dL^{-1} and 21.6 g dL^{-1}. Table 1 shows the conditions of all bioanalytes used in this paper.

Measurement

For measuring the photo-thermal effect, we placed a 10 μL sample on the surface of the micro-fabricated platinum RTD and covered it with a cover glass as shown in Fig. 3(b). The gap between the sensing area and the cover glass was between 100 and 150 μm. We experimented with the photothermal effect of erythrocytes according to the thickness of the blood sample by changing the sample volume. The result shows that the temperature change of erythrocytes is saturated when the thickness of the blood sample exceeds 74.4 μm (6 μL). Over 6 μL of sample volume, additional temperature changes of erythrocytes were not observed. After placing the cover glass on the samples, we set the 532 nm wavelength laser to one of the tested output powers. All of the experiments were performed for three minutes: one minute for stabilizing the sample, one minute for measuring the specimen and one minute for retention.

Results and discussion

Characterization of platinum RTDs

We performed a calibration experiment to verify the sensitivity of the micro platinum RTD. The thermal sensor had a rectangular shaped electrode with a width of 2 μm and a length of 254 μm. The platinum RTDs consisted of 1000 Å-thick platinum with a 200 Å chromium ultra thin layer for adhesion improvement. The resistance of the micro-fabricated platinum RTD at 0 °C was 275.32 Ω. For the characterization of the resistance and sensitivity of the platinum RTD, a J-type (Iron/Constantan) thermocouple (Omega Engineering, INC), Peltier element (Acetec)

and hot plate (Barnstead International) were used (the last two for temperature control). The platinum RTD surface temperature was measured using a J-type thermocouple bonded to the RTD surface and connected to a digital multimeter (Agilent 34970A) for data acquisition. Resistance changes were measured using an *I–V* meter according to the temperature changes of the Peltier element and hot plate. Finally, the temperature change due to the photo-thermal effect was measured. The experiment was carried out at room temperature (23 °C). At the maximum laser intensity of 9.6 W cm^{-2}, we observed a temperature of 30.34 °C. This shows that it is possible to measure the temperature difference of a blood sample because of platinum's low absorbance of 532 nm wavelength light.

Measurement of the photo-thermal effect in reference solutions

Laser-induced heating of the transparent media in living cells has been extensively studied.[15–17] Before measuring the photo-thermal effect of hemoglobin, we measured the temperature changes of cell culture media and buffer solutions using the 532 nm laser source as the baseline. We placed a 10 μL sample on the surface of the micro-fabricated platinum RTD and covered it with a cover glass as shown in Fig. 3(b). After placing the cover glass on the samples, we set the 532 nm wavelength laser to one of the various output powers. DMEM, RPMI, and PBS solution were used, and the results are shown in Table. 1. As the table indicates, the temperature changes of RPMI, DMEM, and PBS at 9.6 W cm^{-2} power and 23 °C were 29.45 ± 1.31 °C, 29.61 ± 1.54 °C, and 30.21 ± 0.68 °C, respectively. Each medium and the buffer solution had a low absorbance for the laser light, causing reflection of the photons. As a result, the temperature changes were insignificant. These levels of change were very small compared to the change for erythrocytes, meaning that the HGB concentration of erythrocyte cultures can be accurately measured using the buffer solution. Although the temperature changes of blood cell media and the buffer solution are proportional to the pulse energy (D_0), D_0 is only one of the determinants of temperature change. All of the experimental results were within an allowable range of error and did not show temperature differences with a 532 nm wavelength and pulse energy.

Measurement of the photo-thermal effects of erythrocytes, leukocytes, and blood plasma

After the reference measurements with the culture media, buffer solution, and bare platinum RTD, erythrocytes, leukocytes, and blood plasma were subjected to laser irradiation, and the temperature changes were measured as described in the experimental section above. Results and photographic images of the erythrocytes are shown in Fig. 4. The hemoglobin concentration of the erythrocyte sample solution was 16.2 g dL^{-1}, and the number of erythrocytes was estimated to be 5.44×10^6 cells μL^{-1}. The temperature changes of the blood plasma, leukocytes, and erythrocytes were 29.89 ± 1.28 °C, 32.24 ± 0.05 °C, and 91.90 ± 5.27 °C at 23 °C (at 9.6 W cm^{-2}), respectively, showing that the erythrocytes had the greatest temperature increase. It was observed that the temperature change of the leukocyte solution was slightly higher than that of blood plasma on its own. This is because a small amount (less than 0.3 g dL^{-1}) of erythrocytes contaminated the buffy coat. Looking at the erythrocyte photographs (Fig. 4), the laser pulse intensity seemed to affect the membrane structure. Hemolysis occurred at 45.5 °C and a 3.2 W cm^{-2} laser pulse intensity. At intensities above 6.4 W cm^{-2}, all erythrocytes were destroyed, as shown in Fig. 4. Although the cellular membranes of the erythrocytes were destroyed, the erythrocytes absorbed much more photon energy than did the plasma, leukocytes, or reference media.

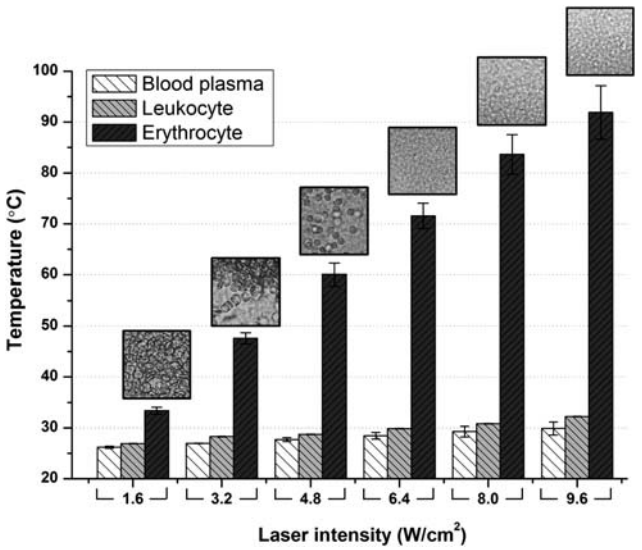

Fig. 4 Temperature changes of erythrocytes, leukocytes and blood plasma. The hemoglobin concentration of the erythrocyte sample solution was 16.2 g dL^{-1}. The photographs of the erythrocytes reflect the gradual hemolysis process caused by photo-thermal heat generation. An intensity of 6.4 W cm^{-2} destroyed all erythrocytes due to disruption of the cell membranes.

After finding that the thermal effect was large enough to measure hemoglobin concentration, we measured the temperature changes of 11 samples with different concentrations. The conditions of the blood samples are shown in Table 1. The experimental conditions were the same as in the previous test. The temperature changes of each sample at different intensities (at 23 °C) are shown in Fig. 5(a). These results indicate that the total amount of thermal energy released by the laser was proportional to the laser pulse intensity and the greater number of input photons leads to greater thermal energy conversion. Also, the total amount of thermal energy increased with the quantity of hemoglobin, indicating that the quantity of light absorbed is proportional to the amount of released thermal energy.

Investigation of the major heat sources in erythrocytes

It is well known that hemoglobin molecules are responsible for absorbing specific wavelengths of light and generating a certain amount of heat.[18] However, it is difficult to know whether the heat detected in our system was truly coming from the major heat source of hemoglobin. We purchased human hemoglobin powder (Sigma-Aldrich) and mixed it with deionized water to make a hemoglobin solution. The concentration of the hemoglobin solution was 8.3 g dL^{-1}, as measured by a conventional

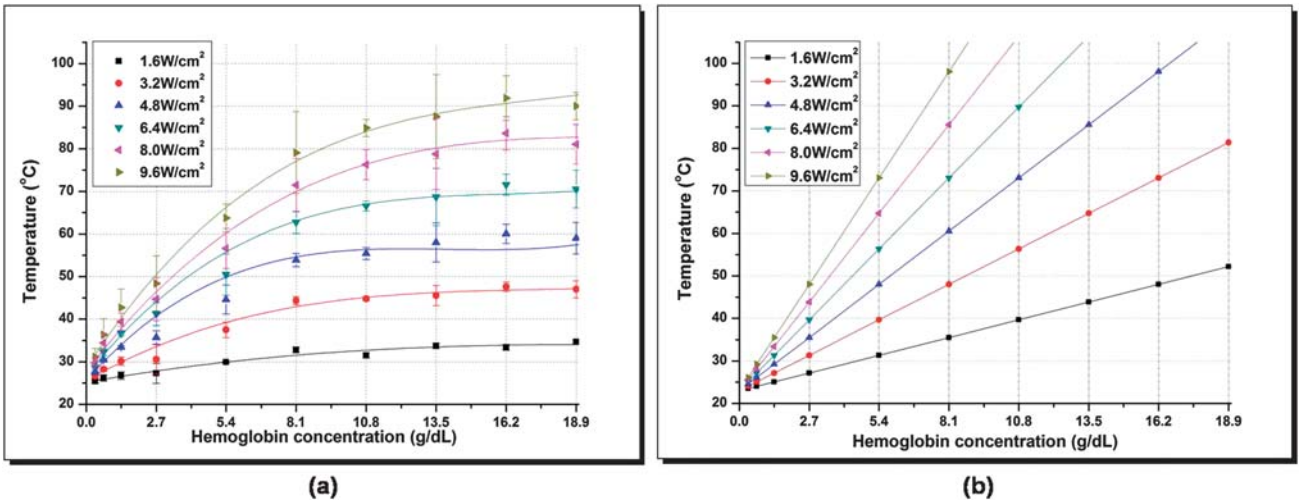

Fig. 5 Temperature changes of red blood cells caused by the photo-thermal effect. (a) Experimental temperature changes (under the conditions used in the analytical calculations). (b) Analytical calculations for temperature changes at different hemoglobin concentrations and laser pulse intensities. The curve fitting equation at 1.6 W cm^{-2} is $0.00045X^3 - 0.04113X^2 + 1.08799X + 25.20191$, $R^2 = 0.97820$; 3.2 W cm^{-2} is $0.00374X^3 - 0.19315X^2 + 3.45677X + 25.58795$, $R^2 = 0.99465$; 4.8 W cm^{-2} is $0.01191X^3 - 0.49669X^2 + 6.81160X + 25.58795$, $R^2 = 0.96239$; 6.4 W cm^{-2} is $0.00950X^3 - 0.45903X^2 + 7.57087X + 26.79324$, $R^2 = 0.99396$; 8.0 W cm^{-2} is $0.00597X^3 - 0.37378X^2 + 7.83337X + 27.85316$, $R^2 = 0.99399$; and 9.6 W cm^{-2} is $0.00933X^3 - 0.49342X^2 + 9.37889X + 28.52592$, $R^2 = 0.99548$.

hemoglobin tester (HemoCue 201$^+$). The temperature increase of the solution was 85 °C at a 9.6 W cm^{-2} laser power, similar to that of the erythrocytes. After testing the hemoglobin solution, we investigated the effect of hemoglobin structure on the photo-thermal effect. We denatured the hemoglobin solution at 70 °C for 10 min and removed the settled and solidified hemoglobin. The hemoglobin concentration of the supernatant was 3.4 g dL^{-1}. For the denatured hemoglobin, the temperature of the solution was 55.44 °C at a 9.6 W cm^{-2} laser power, similar to that for erythrocytes. These results indicate that the three-dimensional structure of hemoglobin is not related to the photo-thermal effect of the erythrocytes. It is known that the photo-thermal effect of erythrocytes is caused by the iron ion in the heme group. We measured the heat properties of iron ions and iron oxide, using a one molar solution of an iron electroplating solution (iron(II) sulfate ($FeSO_4$)) as an iron ion sample and one molar solutions of iron(III) oxide (Fe_2O_3) and magnetite (Fe_3O_4) as iron oxide samples. The temperature of the iron ion, iron(III) oxide, and magnetite samples were 21.92 °C, 63.7 °C and 66.47 °C, respectively, at a 9.6 W cm^{-2} laser power. These results show that iron oxide was the major heat source in the erythrocytes as proved elsewhere.[19]

Comparison of the theoretical calculations and the experimental results

Each erythrocyte contains approximately 270 million hemoglobin molecules. Hemoglobin acts as the main optical absorber and heat source in erythrocytes and is homogenously distributed within the cell volume.[20] Chromophores absorb specific wavelengths of light and convert the light energy to thermal or chemical energy. In 1983, Rox. R Anderson reported on the applications of these phenomena, called "selective photothermolysis",[6] and much emphasis has been placed on healing chromophore-related lesions using the photo-thermal effect. Examples include cutting or reshaping the cornea using an ArF Excimer laser and cutaneous pigmentation curing using a frequency doubled Q-switched Nd:YAG laser. The main variables in this kind of treatment are wavelength (λ), pulse duration (S), and pulse energy (J cm^{-2}). The wavelength (λ) is the main factor in determining photo-thermal efficiency and is a property of the substance being tested. The pulse energy (J cm^{-2}) is related to the temperature changes of the target substrate. The pulse duration (S) is related to the thermal relaxation time (TRT) and is proportional to the thermal damage of the tissue. Because we were focusing on diagnosis instead of treatment, we did not consider the thermal damage to the tissue. Thus, we ignored the pulse duration (S) and used a continuous wave laser.

Using wavelength and pulse energy, we can accurately model the relationship between temperature change and hemoglobin concentration using the following eqn (3)

$$\Delta T = \frac{\Delta E}{\rho S} \tag{3}$$

where ΔE is the energy input per unit volume, ρ is the density, and S is the specific heat of the target choromophore. ΔE is calculated at a specific wavelength of light using eqn (4)

$$\Delta E \cong f\alpha(\lambda)D_0 = fc\varepsilon(\lambda)D_0 \tag{4}$$

where f is the incident intensity decrease factor, $\alpha(\lambda)$ is the light absorption coefficient of the major target chromophore at the specific wave length λ, D_0 is the laser pulse intensity, c is the molar concentration of the target chromophore, and $\varepsilon(\lambda)$ is the milimolar absortivity of the chromophore. The millimolar absorptivity ($\varepsilon_{532\ nm}$) of HbO_2 is 13,000 cm^{-1} M^{-1}.[4] The light absorption coefficient at 532 nm was calculated for each erythrocyte concentration using eqn (4). For these calculations, α (λ = 532 nm, C_{Hb} = 5.4 g dL^{-1}) was 21.45 cm^{-1}, erythrocyte

density (ρ_{RBC}) was 1092 kg m^{-3}, and the heat capacity of blood was 3770J kg^{-1} K^{-1}.[9] The analytical calculation for erythrocyte temperature change is shown in Fig. 5(b). Measuring the temperature changes of hemoglobin at different laser pulse intensities and hemoglobin concentrations leads to the possibility of hemoglobin concentration measurement without pretreatment. The analytical calculation indicates that erythrocyte temperature change is linearly related to laser pulse intensity and hemoglobin concentration. This means that the temperature change of blood samples at a specific laser pulse intensity and wavelength can be used to measure chromophores. The experimental results are similar to the theoretical predictions, though there are some differences, which can be seen in Fig. 5. Fig. 5(a) shows that temperature is converging to a constant value at high hemoglobin concentrations. On the contrary, eqn (4) assumes that all of the energy should be absorbed homogeneously by media with average properties such as density, specific heat and absorption coefficient. There actually exists a mixed phase material of plasma and red blood cells which is dropped between the micro thermal sensor and the cover glass. The cover glass used in this experiments has an area of 9 mm × 9 mm, so we can easily calculate that the thickness of the media can be up to 100 μm in a volume of 10 μL. The local heat is generated between the micro thermal sensor and the cover glass by a 2 mm-diameter laser. We can also neglect lateral conduction through the media because the radial distance from the temperature sensor is much larger than the vertical distance. In addition, the effect of natural convection in liquid media is not significant due to the scale of the liquid phase distance between red blood cells. In these conditions, the higher the concentration of hemoglobin (erythrocytes), the more the particles will be locally distributed on the sensing area. Temperature increases as concentration increases because there are more red blood cells with Fe ions to absorb the photon energy and generate heat. However, when the concentration becomes sufficiently high, there are many particles between the cover glass and the micro thermal sensor. The average distance between red blood cells decreases as concentration increases, becoming less than 2 μm, which is almost the same as the thickness of red blood cells, when the concentration is greater than 10.8 g dL^{-1}. Under higher concentrations, erythrocyes in the upper part of the local heating area may absorb the photon energy and generate heat while at the same time inhibiting those in the lower part. Therefore, at high enough concentrations, the temperature will reach a plateau rather than increasing without bound.

Conclusions

We have demonstrated a new measurement system for determining hemoglobin concentration using a microfabricated thermal sensor and laser irradiation equipment. The temperature increases of erythrocytes are much higher than those of leukocytes, plasma and cell culture media. Our system has several advantages over conventional methods: it can directly measure the quantities of hemoglobin in the blood without inducing hemolysis by chemical treatment; it is relatively simple to implement; and finally, it is cost effective, as no chemicals are needed. We measured temperature alterations of different hemoglobin samples using our micro-fabricated platinum RTD, suggesting that our system can be utilized to diagnose hemoglobin-related diseases. Future work involves single cell analysis to understand the relationship between hemoglobin variations and various disease stages.

Acknowledgements

This work was supported by the "System IC 2010" project of the Korea Ministry of Knowledge Economy (10030554-2008-02), the MOCIE program (a sabbatical grant Y2009 for promoting technological innovation in industry), and the MOEHRD program (KRF-2008-314-D00143). The facilities were provided by KOSEF through the National Core Research Center for Nanomedical Technology (R15-2004-024-00000-0) and ICBIN of Seoul R&BD program (Grant no. 10816).

References

1 Y. K. Park, M. Diez-Silva, G. Popescu, G. Lykotrafitis, W. Choi, M. S. Feld and S. Suresh, *Proc. Natl. Acad. Sci. U. S. A.*, 2008, **105**(37), 13730–13735.
2 F. Ch. Mokken, M. Kedaria, Ch. P. Henny, M. R. Hardeman and A. W. Gelb, *Ann. Hematol.*, 1992, **64**, 113–122.
3 J. Rosenblit, C. R. Abreu, L. N. Szterling, J. M. Kutner, N. Hamerschlak, P. Frutuoso, T. R. Paiva and O. C. Jr. Ferreira, *Sao Paulo Med. J.*, 1999, **117**(3), 108–112.
4 E. J. van Kampen and W. G. Zijlstra, *Adv. Clin. Chem.*, 1983, **23**, 199–257.
5 K. J. Jeon, S. J. Kim, K. K. Park, J. W. Kim and G. W. Yoon, *J. Biomed. Opt.*, 2002, **7**(1), 45–50.
6 R. R. Anderson and J. A. Parrish, *Science*, 1983, **220**, 524–527.
7 D. Lapotko, G. Kuchinsky, H. Antonishina and H. Scoromnik, *Proc. SPIE*, 1996, **2628**, 340–348.
8 D. Lapotko, T. R. Romanovskaya, A. Shnip and V. P. Zharov, *Lasers Surg. Med.*, 2002, **31**, 53–63.
9 D. Lapotko and E. Lukianova, *Int. J. Heat Mass Transfer*, 2005, **48**, 227–234.
10 D. Lapotko, *Lasers Surg. Med.*, 2006, **38**, 240–248.
11 W. A. Clayton, *IEEE Trans. Ind. Appl.*, 1988, **24**, 332–336.
12 G. S. Chung and C. H. Kim, *Microelectron. J.*, 2008, **39**, 1560, DOI: 10.1016/j.mejo.2008.02.028.
13 H. J. Park, J. J. Pak, S. Y. Son, G. B. Lim and I. S. Song, *Sens. Actuators, A*, 2003, **103**, 317–329.
14 P. R. N. Childs, J. R. Greenwood and C. A. Long, *Rev. Sci. Instrum.*, 2000, **71**, 2959–2978.
15 V. P. Zharov, E. I. Galanzha, E. V. Shashkov, N. G. Khlebtsov and V. V. Tuchin, *Opt. Lett.*, 2006, **31**, 3623–3625.
16 V. P. Zharov, E. I. Galanzha and V. V. Tuchin, *Opt. Lett.*, 2005, **30**(6), 628–630.
17 D. Lapotko, *SPIE Newsroom*, 2006, DOI: 10.1117/2.1200603.0156.
18 D. P. Almond, P. M. Patel, *Photothermal Science and Techniques*, Chapman & Hall: London, 1996.
19 J. B. Wittenberg, B. A. Wittenberg, J. Peisach and W. E. Blumberg, *Proc. Natl. Acad. Sci. U. S. A.*, 1970, **67**(4), 1846–1853.
20 D. Lapotko, *Int. J. Heat Mass Transfer*, 2009, **52**, 1540–1543.